Climatic Change
August 2012, Volume 113 (3-4), Pages 563-581
http://dx.doi.org/10.1007/s10584-011-0376-2

Does global warming favour the occurrence of extreme floods in European Alps? First evidences from a NW Alps proglacial lake sediment record

B. Wilhelm[1, 2, *], F. Arnaud[1], D. Enters[1, 3], F. Allignol[1], A. Legaz[1], O. Magand[4], S. Revillon[1, 5], C. Giguet-Covex[1] and E. Malet[1]

[1] Laboratoire Environnement Dynamique et Territoire de Montagne, Le Bourget-du-Lac, France
[2] EDYTEM, Le Bourget-du-Lac, Campus Scientifique, Pôle Montagne, 73 376 Le Bourget-du-Lac, France
[3] GEOPOLAR, Institute of Geography, University of Bremen, Bremen, Germany
[4]Laboratoire de Glaciologie et de Géophysique de l'Environnement, Saint-Martin d'Hères, France
[5] IFREMER, Pouzané, France

*: Corresponding author : B. Wilhelm, email address : bruno.wilhelm@univ-savoie.fr

Abstract:

Flood hazard is expected to increase in the context of global warming. However, long time-series of climate and gauge data at high-elevation are too sparse to assess reliably the rate of recurrence of such events in mountain areas. Here paleolimnological techniques were used to assess the evolution of frequency and magnitude of flash flood events in the North-western European Alps since the Little Ice Age (LIA). The aim was to document a possible effect of the post-19th century global warming on torrential floods frequency and magnitude. Altogether 56 flood deposits were detected from grain size and geochemical measurements performed on gravity cores taken in the proglacial Lake Blanc (2170 m a.s.l., Belledonne Massif, NW French Alps). The age model relies on radiometric dating (^{137}Cs and ^{241}Am), historic lead contamination and the correlation of major flood- and earthquake-triggered deposits, with recognized occurrences in historical written archives. The resulting flood calendar spans the last ca 270 years (AD 1740–AD 2007). The magnitude of flood events was inferred from the accumulated sediment mass per flood event and compared with reconstructed or homogenized datasets of precipitation, temperature and glacier variations. Whereas the decennial flood frequency seems to be independent of seasonal precipitation, a relationship with summer temperature fluctuations can be observed at decadal timescales. Most of the extreme flood events took place since the beginning of the 20th century with the strongest occurring in 2005. Our record thus suggests climate warming is favouring the occurrence of high magnitude torrential flood events in high-altitude catchments.

1. Introduction

During the last decades, noticeable climate changes have been observed at high elevation areas of the European Alps. In-situ observations indicate an increase of the mean annual air temperature of 1 to 2°C and a shift towards drier conditions, but with more intense precipitation events (Beniston et al. 1997; Frei and Schär 2001). However, most high-elevation areas are poorly monitored (Kieffer-Weisse and Bois 2001) and thus spatial and temporal datasets of mean and extreme precipitation rates are insufficient to reveal consistent trends. Furthermore, precipitation pattern and in particular extreme events are poorly simulated by climate models (Jasper et al. 2002; Beniston 2006; Frei et al. 2006) mainly due to complex effects of topography. As a consequence, evidences of changes in extreme events pattern at high altitude remains sparse (Bronstert 2003). While an enhancement of severe flooding hazard is expected within the next decades due to an intensification of the hydrological cycle associated to global warming (Milly et al. 2002; Karl and Trenberth 2003; Huntington, 2006), the question of current and future impact of climatic change on extreme events hence remains an open debate (Huntington 2006). Such issues present a particular public interest as tourism and recent demographic development in the Alps are increasing people and constructions vulnerability to natural hazards (Beniston and Stephenson 2004).

Floods are common and widespread natural hazards. They cause the loss of human life and high cost damage to property and infrastructure and are particularly destructive in mountain areas. For example, in August 2005 a series of catastrophic floods throughout the European Alps caused at least 40 deaths and several billion euros of damage, according to the international press.

To identify the effects of climate change on the frequency and magnitude of flood hazards, historical documents and gauge stations data provide valuable information (e.g. Benito et al. 2004). However, historic descriptions are by nature subjective. In particular, hazard perception by humans varied throughout time and descriptions of damages can thus be biased. Moreover, they may be fragmentary due to destruction or loss and they generally provide only a relatively short time span for analyses, especially in mountain areas. To overcome these limits, natural archives may be used as complementary records (Brazdil et al. 2005).

Among the various natural archives lake sediments have the advantage to be continuous records in which particular events are preserved such as flood events (Siegenthaler and Sturm 1991; Arnaud et al., 2002; Gilli et al. 2003; Boe et al. 2006; Moreno et al. 2008), earthquakes (Chapron et al. 1999; Monecke et al. 2004, Nomade et al. 2005) or debris flows (Irmler et al. 2006). Using lake sediments, it is possible to construct flood calendars covering long-term periods (Nesje et al. 2001; Giguet-Covex et al. 2011) and to assess the magnitude of these events from the thickness or the mass of event-triggered deposits (Irmler et al. 2006; Nesje et al. 2001). In this study, we apply this approach to the sedimentary record of Lake Blanc (Belledonne Massif, NW French Alps). During flood events, coarser particles – coarse silt to fine sand – are carried to the deepest part of the lake where they form characteristic layers. The objective of this study is the reconstruction of a precise flood calendar in order to assess the evolution of frequency and magnitude of flood events at this high elevation environment in the context of global warming.

2. Study area and setting

2.1. Lake Blanc and its catchment

Lake Blanc (2170 m a.s.l., 45°10'42''N, 5°58'21''E) is located five kilometres upstream of the village of Sainte-Agnès in the centre of a small high-altitude cirque of 3 km² (Fig. 1). The geology is dominated by fractured metamorphic rocks (amphibolite and leptynite). Vegetation in the catchment is sparse, only the lower parts being covered by alpine meadows. Due to the high elevation (up to 2977 m a.s.l.) and a favourable orientation, the cirque contains one of the last remaining glaciers of the Belledonne Massif, the Freydane Glacier. Its evolution is well-marked in the landscape by a large proglacial area. In its uppermost part the bedrock appears beneath the currently retreating glacier. Downstream a glacier-fed torrent forms a meandering zone (Fig. 1D). In the lowest part the slope increases and the torrent incises into the basal till and the largest and most distal moraine, attributed to the Little Ice Age (LIA) (Edouard 1994). The morainic material eroded and transported by the river originates essentially from the lowest part of the proglacial area. Some hundred meters downstream the torrent reaches the lake (Fig. 1B). Lake waters remain turbid throughout the thaw period indicating that Lake Blanc receives a continuous and considerable input of glacial flour. A second tributary has a significantly lower discharge and crosses large scree areas without fine particles. Consequently its sedimentary contribution can be assumed to be negligible. From November to May, the catchment area is covered by snow and the lake is frozen, implicating a sediment input only during summer and early autumn.

2.2. The 2005 extreme event and historic floods of the Vorz torrent

On August 21st to 23rd 2005 exceptional meteorological conditions (Grieser et al. 2005) resulted in numerous extreme flood events all over European Alps (Beniston 2006; Böhm and Wetzel 2006; Jaun et al. 2008). In French Alps, several villages located at the foothill of the Belledonne Massif (Fig. 1A) were affected (Prudent-Richard et al. 2008). In particular, in the village of Sainte-Agnès (760 m a.s.l.) the Vorz torrent caused more than 3.2 millions € estimated total damage. Three hydroelectric infrastructures, roads and bridges were destroyed and houses located in the gorge were flooded and filled with sediments (Fig. 1B). This extreme event was triggered by intense precipitations in the highest part of the catchment. A recent rain gauge station located at 2100 m a.s.l. measured about 300 mm-precipitation in 48 h whereas in the same time weather stations in the valley recorded less than 60 mm (Allignol et al. 2008). Within living memory, such a devastating flood event never occurred in Sainte Agnès. As a consequence efforts were undertaken to reconstruct a flood calendar using local and regional historical archives (Allignol et al. 2008). Based on this flood calendar, three events occurred prior to the 20th century with a particularly high impact: one in AD 1851 and two in AD 1852. However ancient land registry indicates only few buildings and reduced land-use of the valley floor of the Vorz. This suggests that the torrent was considered as a potentially hazardous area by that time, which contrasts with the current land-use practice. Therefore, the magnitudes of past and present flood events cannot be directly compared based solely on documental descriptions of damages.

3. Material and methods

3.1. Lake Blanc physical features and sediment cores

In summer 2007, a bathymetric survey was carried out at Lake Blanc and revealed a large subaquatic delta and a flat basin in the centre of the lake with a maximum water depth of 20.3

m. The bathymetric map compared with an aerial photo of 2003 showed also a delta progradation of 15 meters (Fig. 1C). Four short gravity cores (diameter 63 mm and up to 0.5 m. long) were retrieved using an UWITEC coring device from the deepest part of the lake, approximately in the prolongation of the delta (cores BLB0701 and BLB0704) and near the northern slope (cores BLB0702 and BLB0705).

In the laboratory, cores were split, photographed and a detailed description was made to determine the lithological different facies. Half-core BLB0704 was sampled following a 1-cm step and dry at 60°C during four days to obtain dry bulk density. Laser grain size measurements were performed on cores BLB0701, BLB0702 and BLB0704 using a Malvern Mastersizer S following a sampling interval of 0.5 cm. Cross-plots of median grain size (Q50) and the coarse fraction assessed by the particle diameter at the 99-percentile (Q99) of the three facies were used to distinguish and characterize the depositional processes (Passega 1964).

The grain-size data were supplemented by X-ray fluorescence (XRF) measurements which were performed on the ITRAX-XRF core scanner at GEOPOLAR, University of Bremen (Germany) from the core BLB0701 at 1 mm resolution. Relative concentration changes of Ca and Fe, well above the detection limits for this instrument, were used as a complementary approach of the classical grain size measurements to obtain a higher resolution. The use of the Ca/Fe ratio as a high-resolution grain size proxy is based on the assumption that Fe is mostly associated with fine particles, i.e. clays (Cuven et al. 2010) and Ca is more abundant in coarser grain size fractions.

Microstratigraphy was analyzed using impregnated thin sections from cores BLB0701 and BLB0704. For each core five 10-cm long slices were taken with a 2 cm overlap, shock-frozen, freeze-dried and impregnated with Araldite using methods described by Lotter and Lemcke (1999).

3.2. Chronology

In paleoenvironmental studies covering the last century, the age-depth model often relies on the use of ^{210}Pb and ^{137}Cs measurements. Such an approach is not sufficient in our case because the interpretation of ^{210}Pb profiles in high altitude terrigenous-dominated lake sediment is often complex (Arnaud et al. 2002; Guyard et al. 2007). Moreover the precision required for our study is not compatible with a simple extrapolation and interpolation of a measured mean centennial sedimentation rates. Indeed, in such a dynamic sedimentary environment considerable changes in sedimentation rates are expected. Consequently we used additional independent chronological markers in order to build up a reliable, high-resolution age-depth model.

^{137}Cs and ^{241}Am measurements were performed at the LGGE of Grenoble on the upper 25cm of core BLB0704 following a non-regular sampling step of approximately one centimetre, following facies boundaries. This allowed us to locate three chronostratigraphic markers: the fallout of ^{137}Cs originating from atmospheric nuclear weapon tests starting in the northern hemisphere in AD 1955 and culminating in AD 1963 as well as the fallout of ^{137}Cs due to the Chernobyl nuclear plant accident in AD 1986 (Di Lauro et al. 2004). Only the nuclear weapon tests resulted also in a widespread fall-out of ^{241}Pu and the activity of its decay product, ^{241}Am, can now be measured in sediments (Appleby et al. 1991). Thus, a differentiation between the two ^{137}Cs peaks of AD 1963 and AD 1986 layers is possible as only the first one contains ^{241}Am.

Historical lead (Pb) contaminations may also be used as chronostratigraphic markers in sediments (Renberg et al. 2001; Arnaud et al. 2004). Thus, samples of the laminated facies of core BLB0704 (1 cm sampling step) were analyzed for trace elements using conventional XRF method at the IFREMER marine geology laboratory of Brest. To disentangle natural and human-

induced Pb concentration changes Pb concentrations were normalized to the concentration of yttrium (Y), a lithophile element presenting comparable concentration and geochemical behaviour (Faure 1986).

Earthquakes can destabilize and trigger gravity-reworking of slope sediments in lacustrine basins (e.g. Chapron et al. 1999). This results in the deposition of particular layers which can be identified either in the central part of the basin or at the foot step of steep slopes. Linking such gravity-reworked sediment deposits with their respective potential triggering historical seismic event may thus yield additional chronological markers (Arnaud et al. 2002; Nomade et al. 2005; Chapron et al. 2007; Guyard et al. 2007). In order to apply this approach to the sediment record of Lake Blanc we used a method described by Lignier (2001) and subsequently used in Nomade et al. (2005). In a diagram of epicentre-lake distance vs. MSK intensity, epicentres of the major historic earthquakes (represented by points) and the regional seismic intensity propagation (represented by a line) are plotted. The seismic intensity propagation is constructed from two points: the distance to the epicentre of a well-known earthquake and the closest documented point to the lake affected by the same event. Keeping its slope this line is finally adjusted to the number of observed gravity-reworked sediment layers. The adjusted line corresponds to determine the sensitivity of study site in relation to earthquake intensity. This is the minimum seismic intensity causing a gravity-reworking of sediments. The resulting line permits thus to identify earthquakes which were theoretically close or strong enough to trigger gravity-reworking.

The direct downstream position of the village Sainte-Agnès and its abundant historic literature documenting floods events over the last ca. 200 years (Allignol et al. 2008) additionally allowed us to link high-magnitude flood events with particular sediment layers interpreted as flood deposits and add chronological markers similar to approaches described by Blass et al. (2003), Monecke et al. (2004) or Boe et al. (2006).

4. Results

4.1. Sedimentology

All retrieved cores consist of fine-grained laminated sediments in which thicker (max. 1.5 cm) and coarser-grained layers (Fig. 2A) are interbedded. Three lithofacies were identified:

- Facies 1 consists of dark and light, sub millimetre-scale laminae, more or less discernable by eye, with a relative homogenous grain size (mean median grain size: 8.5 µm and mean sorting: 2.6 with standard deviation of 10.5% and 4.8%, respectively).

- Facies 2 is made of dark and thick layers, up to 1.5 cm, sometimes with a visible coarser basal part and always capped by a thin, whitish fine-grained layer. These layers are characterized by a fining upward sequence with a coarser median grain size at the base (27 to 37.7 µm, for cores BLB0704 and BLB0702, respectively) and a finer median grain size (6.9-7.3 µm) than other facies and a global mean sorting of 2.5 and 2.7.

- Facies 3 is a centimetre-scale, sandy matrix-supported layer with a slightly coarser median grain size (12.3 µm) and a significantly higher mean sorting (3.01). This facies was found once in core BLB0702, close to the steep slope.

In the diagram median (Q50) vs. coarser percentile (Q99), samples of facies 1 samples fall in a well-restrained field with a centre defined by a median (Q50) of 8 µm and a coarser percentile (Q99) of 120 µm (Fig. 2B). In contrast, facies 2 and 3 evolve two distinct dynamic patterns. Samples of facies 2 are close to the line Q50 = Q99 which represents a perfect sorting while samples of facies 3 do not show any noticeable variations in the median grain size.

Microstratigraphic observations on thin sections allow a detailed comparison of grain size with the high-resolution Ca/Fe ratio to assess the pertinence of such a ratio as a grain size proxy (Fig. 3). Thin sections scans illustrate the macroscopically described interbedded layers, which are detected from the Ca/Fe ratio. In addition, layers which are too thin to be macroscopically identified, are found on both thin sections and in the Ca/Fe s. A significant correlation (r=0.76, n=20) was found between the median grain size and the 5 mm-resampled Ca/Fe signal for the thickest event-triggered deposits (Fig. 4). For the thinner ones (< 5 mm) no solid relationship was found owing to a dilution effect of the coarsest fraction with the facies 1 during the 5-mm sampling for conventional grain size analysis. Due its high resolution, the Ca/Fe ratio is therefore a more suitable grain size proxy than the classical grain size measurements in this detrital environment.

Finally the stratigraphic correlation of the interbedded layers between the four cores shows the presence of particular deposits only located in some parts of the lake basin (Fig. 2A). Facies 3 has only been observed in one layer in core BLB0702, taken at the foot of the steep northern slope. Furthermore, three distinctive layers of facies 2 are only present in cores BLB0701 and BLB0704 of the deepest part of the lake basin. Two of these layers are consecutive and well-distinguishable at about 8.5 and 9 cm in core BLB0704 but only one was found in the core BLB0701 at about 7 cm. The third layer was identified in cores BLB0701 and BLB0704 at 37.5 and 41 cm, respectively. There are thus altogether four distinctive interbedded layers localized just in some parts of the lake basin, one at the foot of a steep slope (facies 3) and three in the deepest part (facies 2).

4.2. Chronology

The ^{137}Cs record (Fig. 5A) shows a distinct increase of ^{137}Cs activities starting at about 13 cm and culminating with a first peak of more than 300 Bq/kg at 10 cm. A second peak occurs at 7.5 cm depth. The upper part of the profile from 0 to 7 cm is characterized by decreasing activity values. The deepest recorded ^{241}Am activity at 12 cm is also the highest one. Activities of ^{241}Am subsequently decrease towards the top with no detectable activities from 0 to 4 cm. The ^{137}Cs/ ^{241}Am profile shows a regular increase from 12 to 6 cm, disrupted by a sharp depletion at 9 cm corresponding to 2 large interbedded layers.

Values of yttrium (Y) are approximately constant along the core with a mean of 46 ppm and a standard deviation of 2.4 % (Fig. 5B). The lead (Pb) profile has a base level of about 22 ppm with three important peaks. A first increase occurs at the base of the core at 42 to 47 cm sediment depth. A very sharp peak is found at 23-24 cm and a well-marked peak at 8 cm reaches the maximal value of 52 ppm.

Following the method described by Lignier (2001), the regional assessment of the decrease of intensity with the distance from the epicentre was assessed for instance. All historically known earthquakes (Lambert and Levret-Albaret et al. 1996) with an epicentral MSK intensity above V and a maximum distance of 110 km from the lake were carrier forward in intensity vs. distance scatterplot (Fig. 6). The intensity propagation line was then constructed using the well-documented earthquake of Corrençon (AD 1962; Rothe 1972) with a recorded MSK intensity of VIII at the epicentre (38 km distance from the lake) and a MSK intensity of V at Sainte-Agnès which is the closest village from the lake at 5 km distance. By keeping its slope constant this line was then adjusted according to the number of recognized gravity-reworked sediment layers. The resulting line of seismic sensitivity separates potential seismic events which failed to leave an imprint in the sediment record from events triggering gravity-reworked layers, which now can be correlated to the known dates of the events.

5. Discussion

5.1. Triggering mechanisms of different sedimentary deposits

Differences in grain size characteristics (median and sorting) (Fig. 2A) and the different Q50-Q99 patterns (Fig. 2B) allow the differentiation of the three facies into three different depositional processes. The well-restrained field of the facies 1 in the diagram median vs. coarser percentile indicates a sediment deposit of type „pelagic suspension" (Passega 1964). We interpret the facies 1 as the continuous deposit of the regular stream input of glacial flour which led to the steady lake water turbidity. The laminated aspect of facies 1 is then explained by segregation by gravity of particles of different sizes.

The well-sorted facies 2 and the proximity between the facies 2 pattern and the Q99 = Q50 line (Fig. 2B) both suggest that these sediments have been sorted by water currents (Passega 1964; Arnaud et al. 2002), the fining-upward pattern being the results of a decreasing flow velocity. Such particle-loaded currents may have been caused by exceptional floods within the catchment which would significantly increase the turbidity of the water column and lead to the deposition of the thin whitish, fine-grained and well-sorted layer which caps facies 2 sequences. Furthermore the progradation of the whole deltaic shore of about 15 meters observed between 2003 and 2007 represents an increase of 13.5% of the apex-shore distance (Fig. 1C). This fast advance is very likely associated with the major flood event of 2005. This implicates the river spreads over the whole delta during flood events and disperses the sediment over the whole lake basin. The grain size features and the spatial distribution of facies 2 layers are thus coherent, except for the three previously described layers only present in cores BLB0701 and BLB0704. Their grain size characteristics and limited spatial extensions in the deepest part of the lake basin suggest the occurrence of flow deposits originating from delta mass failure (e.g. Shiki et al. 2000). Without the dispersive river current, the reworked sediment flows only downwards the deepest part.

Compared to facies 2, facies 3 is characterized by the absence of a whitish clayey top-level, poorer sediment sorting and a large variation of the Q99 parameter without noticeable median grain size variation. These latter observations confirm the optical description of a matrix-supported layer. This suggests the transport energy is supplied by sediment weight rather than by a water current velocity (Arnaud et al. 2002). Following the nomenclature of Mulder and Cochonat (1996), the so-called facies 3 may thus be interpreted as fluidized flow deposit of reworked sediment originating from a mass failure of the nearest steep slopes as this layer was observed only in the core BLB0702. Lacustrine gravity reworking may be attributed to spontaneous mass failure owing to sediment overloading, rockfall, snow avalanche, lake-level variation or local seismic activity (Monecke et al. 2004). Earthquakes or spontaneous failures seem to be the most probable triggering factors for Lake Blanc as other factors can be excluded for the study site.

Based on the evidences described above, a sedimentological model may be proposed for Lake Blanc. The three kinds of deposits defined above are linked to three triggering mechanisms:

- The deposit of the continuous input of glacial flour constitutes the finely laminated facies 1,

- Major flood events may trigger facies 2 deposits spreaded over the whole lacustrine basin,

- Earthquakes or spontaneous slope failures may have triggered the four spatially discontinuous deposits of facies 2 and 3 deposits by gravity-reworking.

The results from XRF scanning (i.e. Ca/Fe ratio as grain size proxy) were combined with the macroscopic description and conventional grain size measurements in order to establish a complete inventory of flood deposits.

Based on the macroscopical core description, altogether 31 major flood-triggered deposits could be identified. In addition 25 minor flood-triggered deposits were recognized using the Ca/Fe ratio making up a total of 56 floods.

Both the thickness of the flood layer or the accumulated sediment mass could potentially be used to assess the magnitude of each flood event. However bulk density data show an increasing trend with the depth in the first fifteen centimetres indicating some effect of sediment compaction (Fig. 2A). Sediment mass accumulated per event appears thus more suitable than deposit thickness to compare flood magnitude. In this aim accumulated mass per unit of surface (g/cm^2) was assessed for each flood event multiplying the thickness of the deposit (cm) by the dry density (g/cm^3) of the respective sample (Fig. 8A).

5.2. Chronology

5.2.1. Artificial radionuclides

According to the ^{137}Cs and ^{241}Am profiles (Fig. 5), the fallout related to atmospheric nuclear tests started at about 13 cm depth (AD 1955) and culminate with the peak at about 10 cm (AD 1963) which reflects the most active 1961-1962 testing years (UNSCEAR, 2000). The sharp decrease above the peak probably corresponds either to the decrease of atmospheric nuclear tests from 1961-1962 to 1980, or to the reworking of older sediment.

The uppermost activity peak of ^{137}Cs at 7.5 cm, can be attributed to the accident of Chernobyl (AD 1986). The highest value of $^{137}Cs/^{241}Am$ profile is located above the uppermost ^{137}Cs peak and corresponds to a deposit triggered by a flood which may have washed down and concentrated ^{137}Cs Chernobyl fallout.

5.2.2. Historical lead contaminations

Whereas Pb shows significant downcore variations, Y concentrations are relatively constant. This indicates that Pb variations are independent of the accumulation rate variations or rock weathering conditions. Peaks in Pb concentrations can thus be interpreted as atmospheric anthropogenic contaminations. The uppermost peak is situated between AD 1963 and AD 1986 as inferred from the ^{137}Cs peaks (Fig. 5). This recent pollution is likely related to the maximal use of leaded gasoline in years 1973-1974 (e.g. Arnaud et al. 2004).

Older lead pollutions do not correspond to any well-known global contaminations in the literature. Their origin is therefore likely related to local pollution patterns. In the catchment area several old mining sites are known but neither their history nor period of functioning are well-constrained. At the moment we thus can not propose any dates for these older lead contaminations from historical sources.

5.2.3. Identification of historical earthquakes

The four spatially restricted deposits are interpreted as gravity-reworked sediments resulting from the destabilization of delta or lake sides slopes, potentially by earthquakes. Altogether five earthquakes can theoretically be considered to have triggered these four layers (Fig. 1A and 6).

According to Obermeier 1998, Lignier 2001, Monecke et al. 2004 and Nomade et al. 2005, all of them are in the range of intensity (VI-VIII) and distance from the lake (10-40 km) to be able to trigger gravity-reworking. However the earthquake in AD 1839 is uncertain because its epicentre is not clearly defined - between 10 and more than 30 km from the lake (Fig. 6), according to different sources (Rothe 1972). It was therefore not considered in the age-depth model. The two consecutive earthquake-triggered layers localized at 9 cm sediment depth in core BLB0704 can be dated to AD 1962 and AD 1963 which fits well with the ^{137}Cs peak of the atmospheric nuclear tests (Fig. 7). Finally the four earthquakes (AD 1782, 1881, 1962 and 1963) were already recognized as triggers of slope sediment destabilization in the nearby lakes of Laffrey (Nomade et al. 2005), Blanc Huez (Guyard et al. 2007) and Bramant (Chapron et al. 2007). The four observed gravity reworking seem thus clearly be triggered rather by earthquakes than spontaneous slope instabilities owing to sediment overloading.

5.2.4. Historical flood calendar

The uppermost identified flood layer is just below the sediment surface (Fig. 2 and 7). As the cores were retrieved in 2007, it is very likely that this deposit corresponds to the AD 2005 catastrophic flood event. Another large flood damaged the hydroelectric infrastructures and a road in the Vorz catchment in AD 1987. At Sainte-Agnès the discharge was similar as in 2005, but less solid material was mobilized during this event. A corresponding flood event layer was found at 6 cm sediment depth in core BLB0704 (Fig. 7) which fits well with the ^{137}Cs peak of the Chernobyl accident.

To correlate older flood events and their corresponding deposits, we used the flood calendar derived from historical documents in local and departmental archives (Allignol et al., 2008). Seventeen floods impacting the village of Sainte-Agnès are mentioned in these archives since AD 1748 (1748; 1831; 1851; 1852; 1852; 1906; 1912; 1924; 1933; 1939; 1948; 1986; 1987; 1989; 1991; 1996; 2005). After removing floods originating from tributaries other than the Vorz, we used the time constraints given by the historical earthquakes to assign these floods to their particular sedimentary counterparts.

The five floods between AD 1906 and AD 1948 could be allocated to the five flood deposits detected between the earthquakes of Allemond (AD 1881) and Corrençon-en-Vercors (AD 1962) (Fig. 7). The flood deposit associated with the AD 1948 event fits well with the beginning of the ^{137}Cs and ^{241}Am activities from the atmospheric nuclear tests (AD 1950). In the same way we associated the triplet of flood deposits located stratigraphically below the gravity-reworked deposit of "Allemond" (AD 1881) with the three successive historic flood events of AD 1851 and AD 1852 (two events in 1852). The date of AD 1831 was correlated with the last major flood deposit prior to this triplet.

For the 18th century, local archives are very sparse and there is no flood date for the Vorz itself. The older proposed dates (AD 1740, 1748 and 1784) come from departmental archives and concern other rivers. The major flood event of 1784 (Alp'Georisques 2006) happened just after the earthquake of 1782. This flood may thus be associated to the thick deposit directly above the earthquake-triggered deposit. However the absence of continuous sedimentation between the both deposits suggests a very short time between the triggering events (< 1 year) or a sedimentary hiatus. Finally the dates of the two oldest events are based only on the extrapolation of the mean accumulation rate and remain thus uncertain.

Between dated flood deposits, mean sediment accumulation rates (between 0.4 and 2 cm/year for core BLB0701) were calculated in order to interpolate the age-depth model and to date flood

layers which were not recorded in historic documents (Fig. 7). The assigned dates of these floods have an estimated uncertainty of some years (up to +/- 5 years).

5.3. Factors triggering floods

Flood-triggered deposits detected in the Lake Blanc sediment record result from fast and large sediment input owing to exceptional high-magnitude river runoff events which erode, transport and spread the moraine material from the glacier foreland over the whole lake basin. The source of material on one hand and the triggering factors of high river discharge on the other hand are thus the keys for the understanding and the interpretation of the Vorz flood record.

5.3.1. Origin of the material

The main sediment source in this small proglacial catchment is the moraine material, originating essentially from the three large glacier advances of the Little Ice Age (LIA) (Holzhauser et al 2005). A vast quantity of easily erodible detrital matter is thus available since the beginning of the studied period. However only the lowest part of the proglacial area was affected by river erosion. Indeed the main signs of active erosion observed in the field concern the most distal moraine and the basal till just upstream clearly incised without reaching the bedrock (Fig. 1D). These observations suggest the possibility of moraine erosion even when the glacier was occupying its most distal positions at the end of the LIA. In addition basal till can also be eroded and transported by high-magnitude subglacial runoff events during these glacier phases (Benn and Evans 1998, Davies et al. 2003). The tongue of the Freydane glacier was relatively narrow in its lower and middle part owing to the valley morphology, suggesting a subglacial drainage system in dendritic channel network (Ben and Evans 1998). Reported travel times of melt water in this environment are less than two hours for a distance of about two kilometres (Nienow et al. 1998). During flood events the travel time of water from the head catchment to the lake and discharge at the outskirts of the proglacial area can thus be very similar when the glacier was in advanced positions or largely retreated as it is nowadays.

5.3.2. Flood typology

To erode and transport high quantity of material in a short time period, a high-magnitude runoff event is needed. In a small alpine catchment this occurs only during high intensity precipitation (Collins 1998, Merz and Blöschl 2003, Gaume et al 2009). Only for the flood event of 2005 the amount of precipitation was measured at high-elevation by a weather station installed in 2003. The precipitation event lasted mainly two days with a daily rainfall amounts of respectively 174 and 126 mm (> 100-year return period from Gaume et al 2009) and a maximum intensity reaching 9 mm/h. Whereas this event was a large-scale event which affected a great part of central Europe, all others historic Vorz flood events have no analogues in the literature. The high intensity, the isolated character and the summertime of the precipitations triggering Vorz flood events suggest they are usually triggered by local convective events such as thunderstorms (~~"F~~lash Floods" type from Merz and Blöschl 2003).

5.3.3. Flood seasonality

Due to the high altitude, the catchment is covered by snow and the lake is frozen from November to May. During this period intense rainfalls will have virtually no effect on the transport of sediment and potential floods will not be recorded. During spring and early summer the snow and glacial melt feeds the river flow and constitutes a more important sediment input than during late summer and autumn. High changes in mean sediment accumulation rates observed between event-triggered layers can thus be associated to the glacier fluctuations

(Leonard 1986; 1997). However this input contributes to the ~~"~~continuous" sedimentation while the river energy is clearly lower than during flood events *sensu stricto*. According to historic Vorz flood events (Allignol et al. 2008) high intensity precipitations occur preferentially from June to October when the catchment is free of snow-cover. This observation can be extended regionally (Kieffer-Weisse and Bois 2001, Merz and Blöschl 2003; Beniston 2006; Gaume et al. 2009) A rain on snow effect (Collins 1998) on flood events of the Vorz river is thus negligible.

In summary, the moraine material is present in large quantities acting as unlimited sediment supply for at least three centuries and advanced glacier positions were most likely not a significant constraint for transport and erosion throughout the studied period. The main variable in the flood record may be therefore changes in frequency and intensity of flash floods triggered by intense convective precipitation events in summer.

5.4. Global climate context, frequency and magnitude of Vorz flood events

We documented 56 flood events in the Lake Blanc sediment sequence occurring from 1740 to 2007 (Fig. 8A). Our chronicle covers thus two distinct climatic periods; the end of the cold LIA (1740-1860) and the recent warming period (1860-2007).

5.4.1. Flood frequency

There is no distinction in flood occurrence between these two periods; 27 events (mean return period: 4.5 years) vs. 29 respectively (mean return period: 5 years). Three significant periods without any flood occurrence are noticeable: 1750-1775, during the L.I.A., 1870-1905 and 1960-1985 during the recent warming. Similarly periods of high flood frequency occurred during the LIA (1790-1805 and 1830-1845) as well as during the 20th century (1905-1915 and 1945-1960) with a similar frequency of 5-7 events per 11 years.

5.4.2. Flood intensity

The magnitude of the flood events was assessed from the quantity of material deposited per event. The most important deposits (~ 1 g.cm^{-2}) are consecutive and respectively associated to the 1782 historic earthquake and to the 1784 historic flood. The delta slope destabilisation following the earthquake may have disturbed the delta sedimentation pattern and resulted in a bias in the transported/deposited sediment during the ~~"~~1784" flood event. The inferred magnitude of the ~~"~~1784" flood event is thus associated with a high uncertainty. Others distinct flood deposits (> 0.8 g.cm^{-2}) were in decreasing order of magnitude (1784) 2005, 1906, 1987, 1933. All the strongest ones occurred thus during the recent warming period (20th century). Furthermore the 2005 flood event, felt by local residents to be an exceptional event, is indeed the strongest one (1 g.cm^{-2}) for at least the last two centuries or even maybe from the whole studied period. This result is supported by the observed delta progradation as well as the measured daily precipitation assessed to be much higher than the expected 100-yrs return period event (Gaume et al. 2009). Furthemore the flood of 1987 is assessed to be a catastrophic event (0.89 g.cm^{-2}) but less strong than the 2005 one, which is in agreement with the description of inhabitants.

5.5. Flood hazard evolution in the context of recent, current and future global climatic change

Flood events in the Vorz catchment are triggered by local, short but high intensity rainfalls. In the absence of long-term meteorological data from the catchment area, we use precipitation and temperature data derived from homogenised instrumental dataset covering almost the whole studied period (1760-2008) and the studied region (Histalp dataset; Auer et al. 2007). Monthly precipitation and temperature data permit to characterise climatic conditions favourable for triggering flood events. Summer dryness vs. wetness can be assessed from the mean June, July and August precipitations and temperature data (Fig. 8B). Furthermore glacier fluctuations are also shown as a high-elevation climate proxy (Intergovernmental Panel on Climate Change 2001) (Fig. 8C). The glacier of Bossons (Massif de Chamonix / Mt. Blanc, ca. 100 km north-east from the study site) was chosen due to its fast response time to climate fluctuations. Glacier front variability shows two advances (1760-1780 and 1805-1820) before the large retreat initiated at the end of the LIA, punctuated by weaker advances (1875-1895 and 1950-1980). The three periods without flood activity in Lake Blanc (1750-1775, 1870-1905 and 1960-1985) correspond to these advance phases. During the first part of the studied period the Freydane glacier reached the most distal LIA glacier position. The absence of flood activity during this phase could thus be interpreted as an effect of the extended ice cover. However, we argued previously that erosion of the basal till and the steep and most distal moraine (older than the LIA) was always possible. Furthermore a comparable period without any flood event occurred in the 60's when the glacier was largely retreated upstream the incised area. We thus interpret these contemporaneous phases of glacier advance and of reduced flood activity as distinct responses to a particular climate pattern, characterized here by colder temperatures. Inversely periods of high flood frequency (1790-1805, 1830-1845, 1945-1960, 1905-1915, 1985-2007) seems to be associated with periods of higher temperatures. The most recent increase of high intensity precipitation events since the mid-80's is documented in the region by Jomelli et al. (2007). The temperature-flood frequency relationship is based on the assumption that higher temperatures can theoretically trigger more high intensity rainfall (Trenberth 1999, Huntington 2006). However time-lags of 5 to 10 years are observed between warming and increase of flood frequencies, following the two very cold flood-free periods (1805-1820 and 1875-1890), respectively. This may be attributing to the time-lag necessary to unfreeze the periglacial permafrost which protects the moraine material from erosion. Such behaviour hasbeen documented for high elevation debris flow studies (e.g. Rebetz et al. 1997, Jomelli et al. 2007). According to the described altitudes (up to 2300-2400 m a.s.l.) of the current or past permafrost (Haeberli 1975, Rebetz et al. 1997, Jomelli et al. 2007) the proglacial area might have been affected by the permafrost during these extreme periods. In the recent period of global warming some studies report a decrease of total rainfall amounts but with higher intense events (e.g. Beniston et al. 1997; Frei and Schär 2001). Summer precipitation and Vorz floods triggered by high intensity events were compared trying to evidence such a relationship. However summer precipitations show no significant relation with the flood frequency and/or magnitude (Fig. 8). Finally, despite a significant temperature increase since the 80s, the flood frequency presents only a slight increasing trend compared to the first half of the 20th century. This lower frequency might be a precursory trend of the decrease in summer flood frequency and associated with a seasonal shift of extreme precipitation from summer to spring.

6. Conclusion

This paper focuses on the evolution of flash floods at high elevation from both natural and historical archives. The study of lacustrine sediments permitted us to reconstruct a detailed flood calendar for the last 270 years based on independent dating methods. The magnitude of each event has been assessed from the quantity of material deposited per event in the lake. The obtained flood calendar reports 56 floods over the last 270 years with an assessed magnitude ranging from 0.1 to 1.1 g.cm^{-2}. Only 17 of these floods are mentioned in historical

documents with no unbiased indication of their magnitude.The paleolimnological approach appears thus as an excellent way to assess both frequency and magnitude of flash flood activity in mountainous regions where instrumental records are rare and extreme precipitation patterns can only poorly be modelled.

The comparison of the obtained flood calendar with alpine temperature and precipitation data as well as glacier fluctuations suggests a relationship between climatic change and the evolution of torrential activity. No relationship was found with long-term precipitation records but a complex relationship with temperature seems to exist. No general trend appears between the end of the LIA and the 20th century but the flood frequency increases on a decadal timescale during warming periods, whereas virtually no floods are recorded during glacier advances. After the coldest periods time-lag of flood activity increase occurred, suggesting the temporary presence of the permafrost conditions. This could have weakened the efficiency of erosion processes during high precipitation events. We showed that the probability of occurrence for extreme flood events increased with a long term temperature rise. Among the 7 extreme flood events, 4 occurred during the 20th century, but they are ranked as the most extreme ones. In particular, the 2005 event is the strongest of the whole considered period. These results support the hypothesis of an increase of heavy rainfall events due to the enhancement of the hydrologic cycle in the context of global warming.

The presented results are restricted of a relatively small area and therefore give only a local signal of precipitation changes. In order to obtain a more regional climate evolution, several other (proglacial) lakes are currently studied. These data will improve and constrain our understanding of the relationship between climatic change and devastating flood events.

Acknowledgments

B. Wilhelm's work is supported by a grant from the Assemblée des Pays de Savoie and the Communauté de Communes des Balcons de Belledonne. Logistical and financial supports were brought in the framework of the scientific programmes Vorz, founded by the Communauté de Communes des Balcons de Belledonne and Pygmalion, founded by the French National Research Agency (ANR BLAN07-2_204489). Authors are particularly grateful to the Sainte Agnes' mayor who launched the Vorz programme and brought valuable help for field campaigns. Authors are grateful to Prof. Bernd Zolitschka who kindly permitted the access to the Geopolar XRF core scanner device and to the database Histalp which permits to obtain free climatological long series (http://www.zamg.ac.at/histalp). Thin sections were performed thanks to the technical facilities of the ~~-~~plateforme d'analyses structurales et environnementales" (ASTRE) of the University of Savoie.

References

Allignol F, Arnaud F, Champagnac J.D, Delannoy JJ, Deline P, Fudral S, Paillet A, Ployon E, Ravanel L, Saulnier GM, Wilhelm B (2008) Etude intégrée du bassin versant du Vorz (Belledonne, Isère) consécutive à la crue des 22 et 23 août 2005. Rapport scientifique, Laboratoire EDYTEM, Le Bourget du Lac, 202 p.

Appleby PG, Richardson N, Nolan PJ (1991) 241Am dating of lake sediments. Hydrobiol 214:35–42

Arnaud F, Lignier V, Revel M, Desmet M, Pourchet M, Beck C, Charlet F, Trentesaux A, Tribovillard N (2002) Flood and earthquake disturbance of 210Pb geochronology (Lake Anterne, North French Alps). Terra Nova 14;225–232

Arnaud F, Revel-Rolland M, Winiarski T, Chapron E, Desmet M, Tribovillard N, Givelet N (2004) History of lead contamination in Northern French Alps from distant lake sediment records, J Environ Monit 6:448-456

Auer I, Böhm R, Jukovic A, Lipa W, Orlik A, Potzmann R, Schöner W, Ungersböck M, Matulla C, Briffa K, Jones P, Efthymiadis D, Brunetti M, Nanni T, Maugeri M, Mercalli L, Mestre O, Moisselin JM, Begert M, Müller-Westermeier G, Kveton V, Bochnicek O, Stasny P, Lapin M, Szalai S, Szentimrey T, Szentimrey T, Cengar T, Dolinar M, Gajic-Capka M, Zaninovic K, Majstorovicp Z, Nieplovaq E (2007) HISTALP – historical instrumental climatological surface time series of the Greater Alpine Region. Int. J. Climatol. 27:17–46

Benn DI and Evans DJA (1998) Glaciers and Glaciation. Edward Arnold, London.734 pp.

Beniston M, Diaz HF, Bradley RS (1997) Climatic change at high elevation sites: an overview. Clim. Change 36:233 - 251

Beniston M (2006) August 2005 intense rainfall event in Switzerland: Not necessarily an analog for strong convective events in a greenhouse climate. Geophys Res Letters 33;L05701

Beniston M, Stephenson DB (2004) Extreme climatic events and their evolution under changing climatic conditions. Glob Planet Change 44:1-9

Benito G, Lang M, Barriendos M, Llasat MC, Francés F, Ouarda T, Thorndycraft VR, Enzel Y, Bardossy A, Coeur D, Bobée B (2004) Use of Systematic, Palaeoflood and Historical Data for the Improvement of Flood Risk Estimation, Review of Scientific Methods. Nat Hazards 3:623–643

Blass A, Anselmetti FS, Ariztegui D (2003) 60 years of glaciolacustrine sedimentation in Steinsee (Sustenpass, Switzerland) compared with historic events and instrumental meteorological data, Eclogae Geol Helv 96(1):59–71

Boe AG, Olaf Dahl S, Lie O, Nesje A (2006) Holocene river floods in the upper Glomma catchment, southern Norway: a high-resolution multiproxy record from lacustrine sediments. The Holocene 16(3):445-455

Böhm O, Wetzel KF (2006) Flood history of the Danube tributaries Lech and Isar in the Alpine foreland of Germany. Hydrol Sci J 51(5):784-798

Brazdil R, Pfister C, Wanner H, Von Storch H, Luterbacher JR (2005) Historical climatology in Europe – the state of the art. Clim change 70:363–430

Bronstert A (2003) Floods and Climate Change: Interactions and Impacts, Risk Anal 23(3):545-557

Chapron E, Beck C, Pourchet M, Deconinck JF (1999) 1822 earthquake-triggered homogenite in Lake Le Bourget (NW Alps). Terra Nova 1:86-92

Chapron E, Faïn X, Magand O, Charlet L, Debret M, Mélières MA (2007) Reconstructing recent environmental changes from proglacial lake sediments in the Western Alps (Lake Blanc Huez, 2543 m a.s.l., Grandes Rousses Massif, France). Palaeogeogr Palaeoclimatol Palaeoecol 252; 586–600

Coeur D (2003) La maîtrise des inondations dans la plaine de Grenoble (XVIIe-XXe siècle) : enjeux techniques, politiques et urbains. Thèse soutenue à l'University Pierre Mendès France de Grenoble

Collins D (1998) Rainfall-induced high-magnitude runoff events in highly-glacierized Alpine basins. Hydrol., Water Resour. and Ecol. in Headwaters. IAHS Publ. 248:69-78

Cuven S, Francus P, Lamoureux S (2010) Estimation of grain size variability with micro X-ray fluorescence in laminated lacustrine sediments, Cape Bounty, Canadian High Arctic. J Paleolimnol 44(3):803-817

Davies TRH, Smart CC, Turnbull JM (2003) Water and sediment outbursts from advanced Franz Joseg glacier, New Zealand. Earth Surf. Preocess. Landforms 28:1081-1096

Di Lauro A, Fernex F, Fierro G, Ferrand JL, Pupin JP, Gasparro J (2004) Geochemical approach to the sedimentary evolution of the Bay of Nice (NW Mediterranean sea). Cont Shelf Res 24;223–239

Edouard JL (1994) Les lacs d'altitude dans les Alpes françaises, contribution à la connaissance des lacs d'altitude et à l'histore des milieux montagnards depuis la fin du Tardiglaciaire. Thèse soutenue à l'University J. Fourier de Grenoble

Faure G (1986) Principles of isotope geology. John Wiley & Sons, New York. 286 pp.

Frei C and Schär C (2001) Detection probability of trends in rare events: theory and application to heavy precipitation in the alpine region. J. Clim. 14:1568-1584

Frei C, Schöll R, Fukutome S, Schmidli J, Vidale PL (2006) Future change of precipitation extremes in Europe: Intercomparison of scenarios from regional climate models, J Geophys Res-Atm 111, D06105, DOI: 10.1029/2005JD005965

Gaume E, Bain V, Bernardara P, Newinger O, Barbuc M, Bateman A, Blaškovicˇová L, Blöschl G, Borga M, Dumitrescu A, Daliakopoulos I, Garcia J, Irimescu A, Kohnova S, Koutroulis A, Marchi L, Matreata S, Medina V, Preciso E, Sempere-Torres D, Stancalie G, Szolgay J, Tsanis I, Velasco D, Viglione A (2009) A compilation of data on European flash floods. J Hydrol 367:70–78

Giguet-Covex C, Arnaud F, Poulenard J, Disnar JR, Delhon C, Francus P, David F, Enters D, Rey PJ, Delannoy JJ (2011) Changes in erosion patterns during the Holocene in a currently treeless subalpine catchment inferred from lake sediment geochemistry (Lake Anterne, 2063 m asl, NW French Alps): the role of climate and human activities. The Holocene doi:10.1177/0959683610391320

Gilli A, Anselmetti FS, Ariztegui D, McKenzie JA (2003) A 600-year sedimentary record of flood events from two sub-alpine lakes (Schwendiseen, Northeastern Switzerland). Eclogae Geol Helv 96(1):49-58

Grieser J, Beck C, Rudolf B (2005) The Summer Flooding 2005 in Southern Bavaria – A Climatological Review. Klimastatusbericht 2005:168-173

Guyard H, Chapron E, St-Onge G, Anselmetti FS, Arnaud F, Magand O, Francus P, Melières MA (2007) High-altitude varve records of abrupt environmental changes and mining activity over the last 4000 years in the Western French Alps (Lake Bramant, Grandes Rousses Massif), Quat Sci Rev 26:2644-2660

Haeberli W (1975). Untersuchungen zur Verbreitung von Parmafrost zwischen Flüelapass und Piz Grialetsch (Graubünden). Mitteilung der Versuchsanstalt für Wasserbau, Hydrologie und Glaziologie an der Eidgenössischen Technischen Hochschule Zürich, 17, 221 p.

Holzhauser H, Magny M, Zumbühl HJ (2005) Glacier and lake-level variations in west-central Europe over the last 3500 years. The Holocene 15(6):789-801

Huntington TG (2006) Evidence for intensification of the global water cycle: Review and synthesis. J Hydrol 319:83-95

Intergovernmental Panel on Climate Change (2001), Climate Change: Contribution of Working Group I to the Third Assessment Report of the Intergovernmental Panel on Climate Change, Cambridge Univ. Press, New York.

Irmler R, Daut G, Mäusbacher R (2006) A debris flow calendar derived from sediments of lake Lago di Braies (N. Italy). Geomorphol 77:69–78

Jaun S, Ahrens B, Walser A, Ewen T, Schär T (2008) A probabilistic view on the August 2005 floods in the upper Rhine Catchment. Nat Hazards Earth Syst Sci 8:281–291

Jasper K, Gurtz J, Lang H (2002) Advanced flood forecasting in Alpine watersheds by coupling meteorological observations and forecasts with a distributed hydrological model. J Hydrol 267:40-52

Jomelli V, Brunstein D, Grancher D and Pech P (2007) Is the response of hill slope debris flows to recent climate change univocal? A case study in the Massif des Ecrins (French Alps). Clim Change 85:119–137

Karl T.R, Trenberth K.E (2003) Modern Global Climate Change. Sci 302:1719-1723

Kieffer-Weisse A and Bois P (2001) Estimation de paramètres statistiques des précipitations extrêmes dans les Alpes françaises. La Houille Blanche 1:62-70

Lambert J, Levret-Albaret A (1996) Mille ans de séismes en France. Ouest Editions, Nantes, 79 pp.

Leonard EM (1986) Use of lacustrine sedimentary sequences as indicators of Holocene glacial history, Banff National Park, Alberta, Canada. Quat Res 26: 218- 231

Leonard EM (1997) The relationship between glacial activity and sediment production; evidence from a 4450-year varve record of neoglacial sedimentation in Hector Lake, Alberta, Canada. J Paleolimnol 17(3): 319-330

Lignier V (2001) Les sédiments lacustres et l'enregistrements de la paléosismicité, étude comparative de différents cas dans le Quaternaire des Alpes Nord-Occidentales et du Tien-Shan Kyrghyze. Thèse soutenue à l'University de Savoie

Lotter AF, Lemcke G (1999) Methods for preparing and counting biochemical varves. Boreas 28(2):243-252

Merz R and Blöschl G (2003) Regional flood risk—what are the driving processes? Water Resour. Syst.- Hydrol. Risk, Manag. and Dev. IAHS Publ. 281:49-58

Milly PCD, Wetherald RT, Dunne KA, Delworth TL (2002) Increasing risk of great floods in a changing climate. Nat 415:514-517

Monecke K, Anselmetti FS, Becker A, Sturm M, Giardini D (2004) The record of historic earthquakes in lake sediments of Central Switzerlanc. Tectonophysics 394: 21-40

Moreno A, Valero-Garcés BL, Gonzales-Sampériz P, Rico M (2008) Flood response to rainfall variability during the last 2000 years inferred from the Taravilla Lake record (Central Iberian Range, Spain). J Paleolimnol 40:943–961

Mulder T, Cochonat P (1996) Clasification of offshore mass movements. J Sedimentol Res 66(1);43-57

Nesje A, Olaf Dahl S, Matthews JA, and Berrisdorf MS (2001) A ~4500 years of river floods obtained from a sediment core in Lake Atnsjoen, eastern Norway. J Paleolimnol 25;329-342

Nienow P, Sharp M, Willis I (1998) Seasonal changes in the morphology of the subglacial drainage system, Haut Glacier d'Arolla, Switzerland. Earth Surf. Process. Landforms 23:825-843

Nomade J, Chapron E, Desmet M, Reyss JL, Arnaud F, Lignier V (2005) Reconstructing historical seismicity from lake sediments (Lake Laffrey, Western Alps, France). Terra Nova 17: 350-357

Obermeier SF (1998) Liquefaction evidence for strong earthquakes of Holocene and latest Pleistocene ages in the states of Indiana and Illinois, USA. Engineering Geology 50: 227–254

Passega R (1964) Grain-size representation by CM patterns as a geological tool. J Sediment Petrol 34(4), 830-847

Prudent-Richard G, Gillet M, Vengeon JM, Descotes-Genon S (2008) Changements climatiques dans les Alpes : Impacts et risques naturels. Rapport Technique de l'O.N.E.R.C., 99 pp

Rebetz M, Lugon R, Baeriswyl PA (1997) Climatic change and debris flows in high mountain regions: the case study of the Ritigraben Torrent (Swiss Alps). Clim.Change 36: 371–389

Renberg I, Bindler R, Bränvall ML (2001) Using the historical atmospheric lead-deposition record as a chronological marker in sediment deposits in Europe. The Holocene 11(5):511-516

Rothe E (1972) Annales de l'Institut de Physique du Globe, 3e Partie géophysique. T. IX, University Louis Pasteur, 134 pp.

Siegenthaler C, Sturm M (1991) Die Häufigkeit von Ablagerungen extremer Reuss-Hochwasser. Die Sedimentationsgeschichte im Urnersee seit dem Mittelalter, In: Ursachenanalyse der Hochwasser 1987. Ergebnisse der Untersuchungen. Mitteilungen des Bundesamtes für Wasserwirtschaft 4:127-139.

Shiki T, Kumon F, Inouchi Y, Kontani Y, Sakamoto T, Tateishi M, Matsubara H, Fukuyama K (2000) Sedimentary features of the seismo-turbidites, Lake Biwa, Japan. Sedimentary Geology 135:37-50

Trenberth KE (1999) Conceptual framework for changes of extremes of the hydrological cycle with climate change. Clim Change 42:327-339

UNSCEAR (2000) United Nations Scientific Committee on the Effects of Atomic Radiation, Sources and Effects of Ionizing Radiation. In: Report to the General Assembly (ed) United Nations, New-York, Annex C, exposures to the public from man-made sources of radiation, pp 158-291

Vincent C, Le Meur E, Six D, Funk M (2005) Solving the paradox of the end of the Little Ice Age in the Alps. Geophys res lett 32, L09706, doi:10.1029/2005GL022552

Figures

Figure 1. Geographical setting of the study area and location of investigated lacustrine sediment archive. (A) Location of the study area (star) in the Belledonne Massif in French Alps and historical earthquakes (circles) with their respective dates and MSK intensities (roman numerals) (Lambert and Levret-Albaret 1996). (B) The main damages on the surrounding area of Sainte-Agnès triggered by the Vorz Torrent during the 2005 flood event and location of Lake Blanc catchment area (red and dash line) in the Vorz head catchment. The LIA moraine just upstream of Lake Blanc is indicated by a dotted line. (C) Bathymetry of Lake Blanc, location of the four studied sediment cores and zoom in the delta evolution in the right and low part. (D) Details of the Vorz Torrent characteristics (profile, slope and morphologies) in the Lake Blanc catchment.

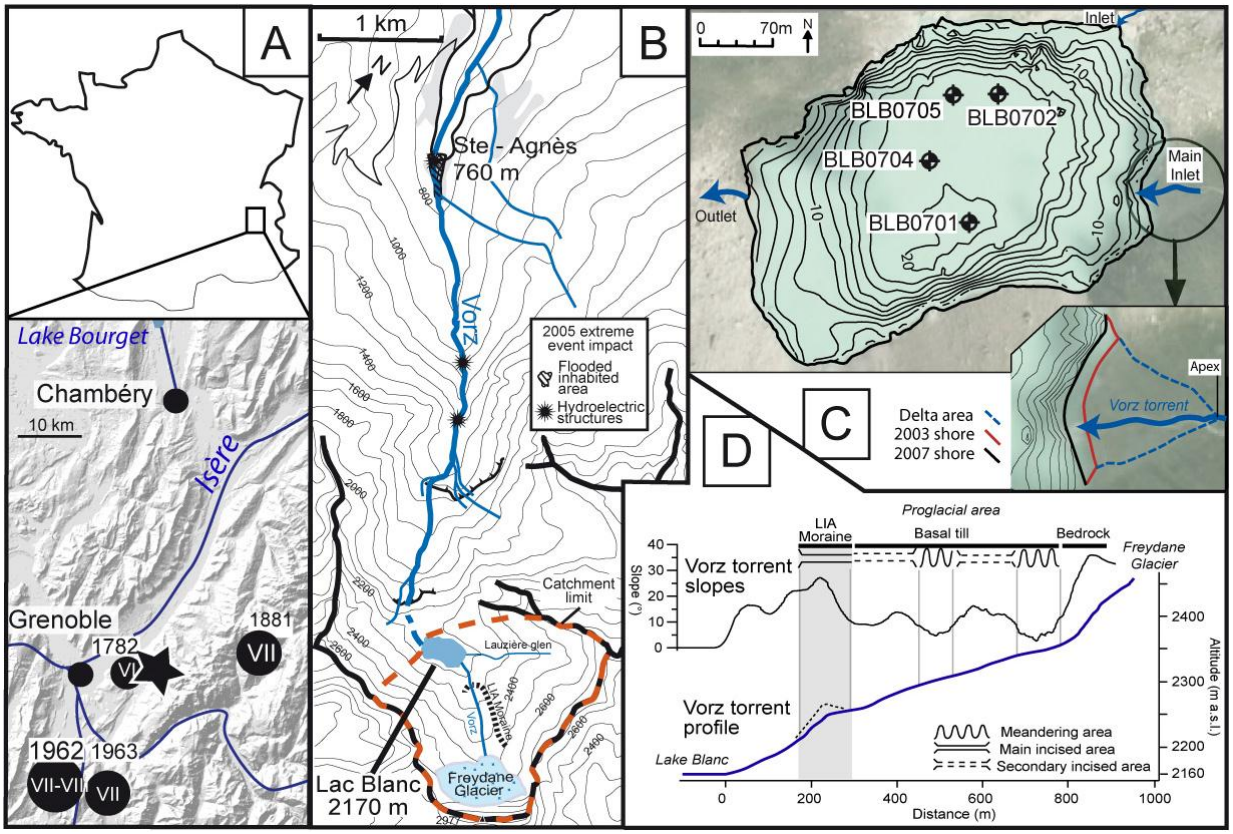

Figure 2. (A) Lithology, down core grain size characteristics of BLB0701, BLB0702 and BLB0704 and dry bulk density of BLB0704. (B) Q99 vs. Q50 plots of samples from the same cores

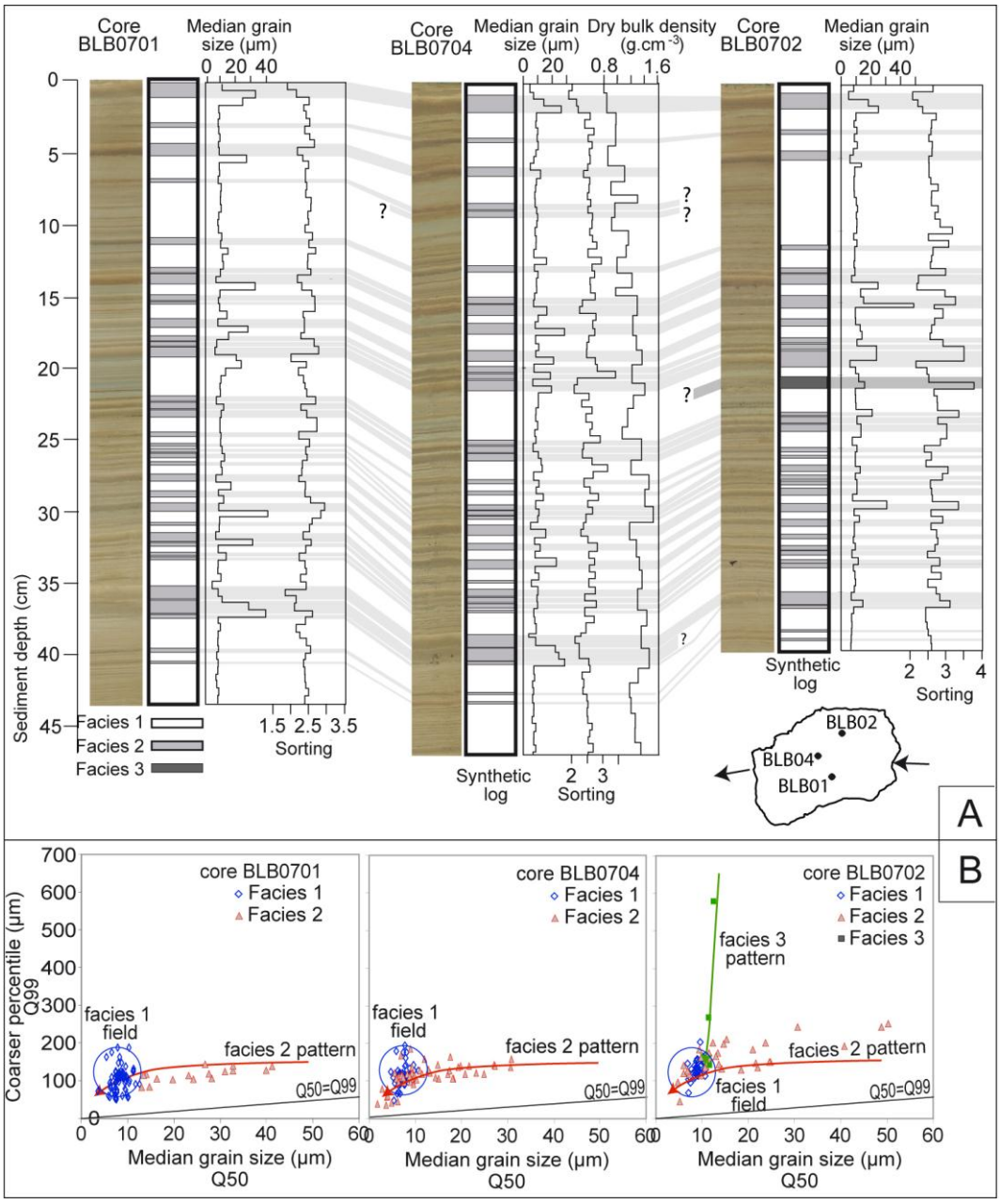

Figure 3. Mean grain-size, raw 1-mm Ca / Fe ratio and scans of thin sections of the core BLB0701. Grey bars through the plots indicate event-triggered deposits determined by the both methods (for more explanation, see text). The hole in the lowest thin section resulted from an insufficient impregnation of the sediment

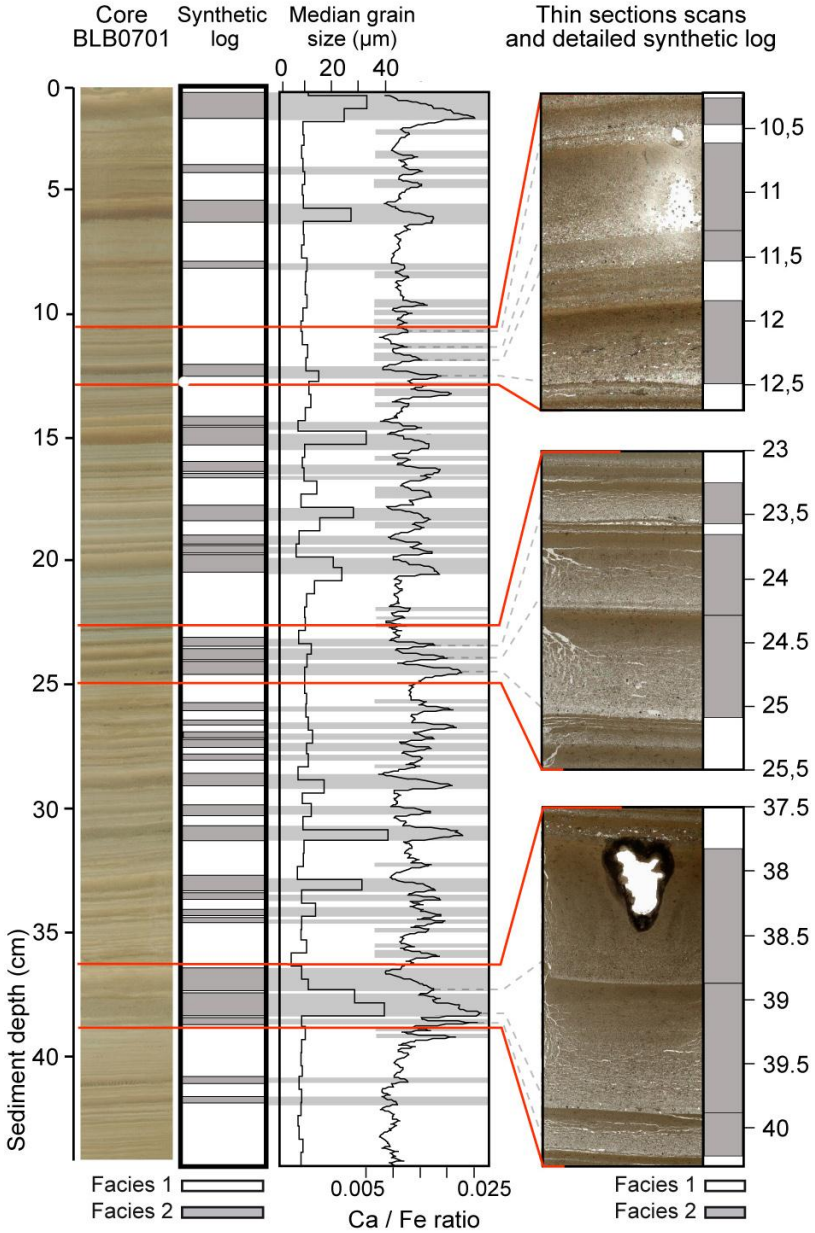

Figure 4. Cross-plot of the median grain size vs. the 5 mm-resampled Ca/Fe signal from BLB0701 data and linear regression for samples of event-triggered deposits thicker than 5 mm.

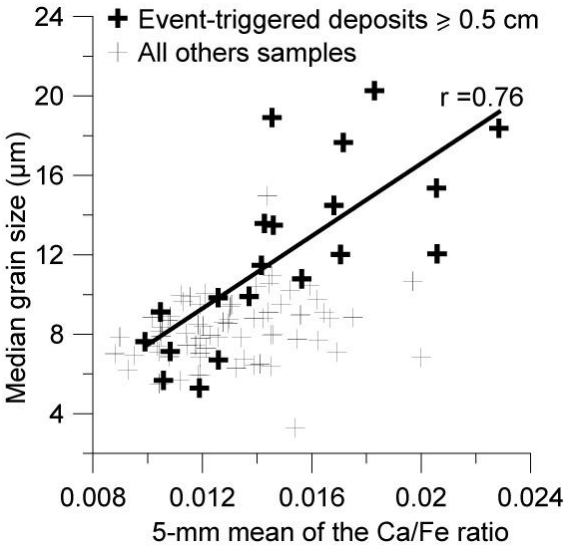

Figure 5. Radionuclides and geochemical chronostratigraphic indicators from core BLB0704. (A) ^{137}Cs, ^{241}Am and $^{137}Cs/^{241}Am$ profiles. (B) Lead concentration profile, normalized by yttrium, permits to detect anthropogenic contamination (shaded zones).

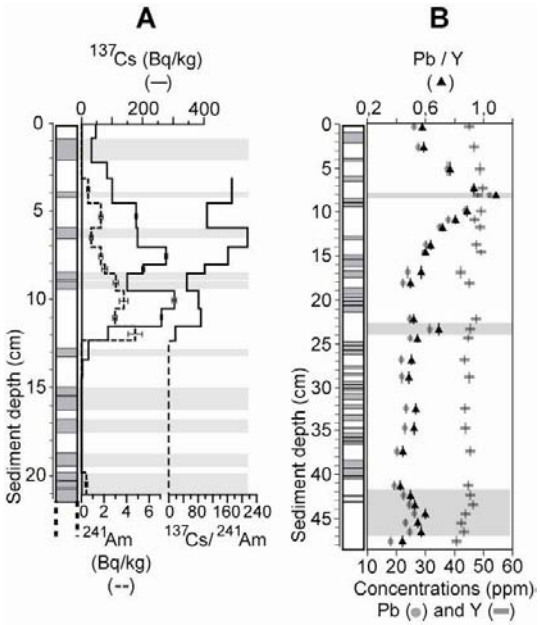

Figure 6 Plot of historic earthquakes in the vicinity of Lake Blanc (MSK intensity > V and distance < 110 km) in an intensity vs. distance diagram. The seismic sensitivity line permits to distinguish potential earthquakes susceptible to trigger gravity reworking from all historic earthquakes.

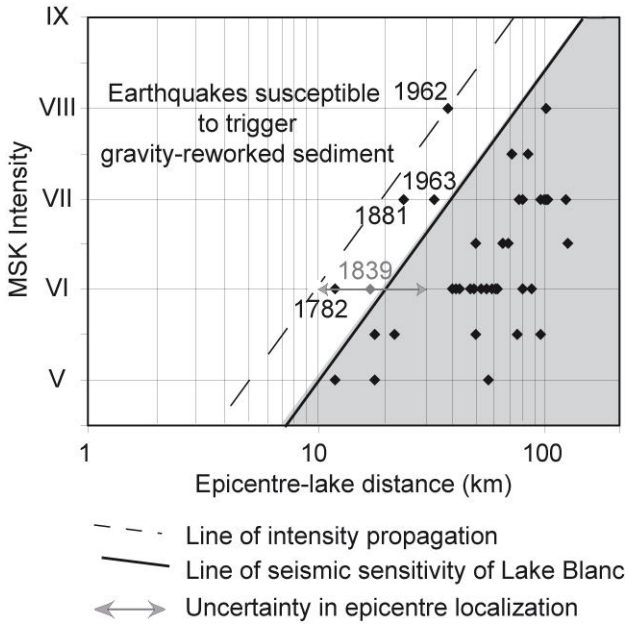

Figure 7. Age-depth relationship for core BLB0704 established from detected periods of radioactive (red) and lead (green) global pollutions and historically documented earthquakes (yellow) and floods (blue). For explanation about origin of the dates, see the text.

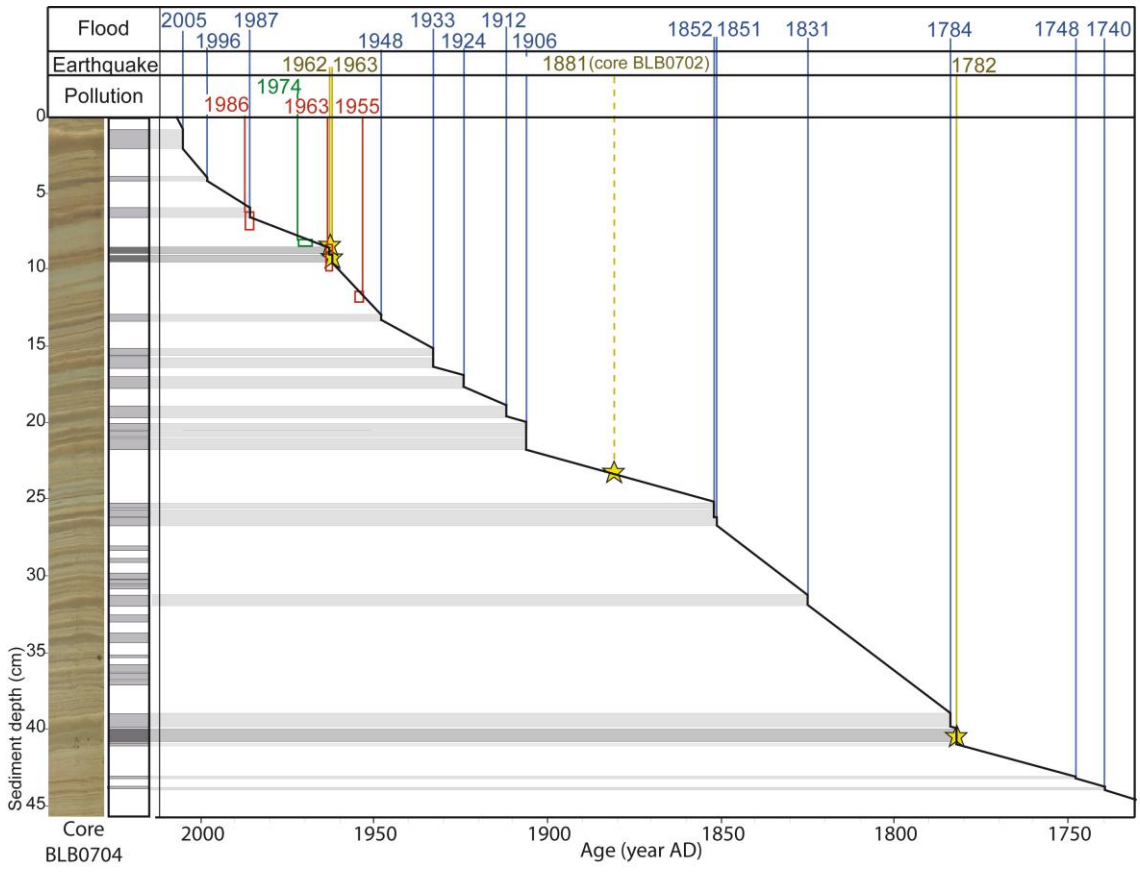

Figure 8. Calendar of the 56 Vorz flood deposits, respective mass accumulated per event and flood frequency (A) compared with instrumental long series (B) and the fluctuations of the Glacier of Bossons (C). Each bar of the flood calendar represents one individual flood deposit and the size of the bar its deposit mass accumulated per unit of surface and per event, interpreted here as the magnitude of the flood event. The shaded zones correspond to the long-lasting periods of glacier advance.